PRACTICAL FIXED-TIME CONSENSUS IN STOCHASTIC DISCRETE-TIME MULTI-AGENT SYSTEMS UNDER A NONLINEAR LOCAL VOTING PROTOCOL

Daniil Mingazov
IT Department
TltGames Studio
Russia
daniilmingazov@mail.ru

Olga Granichina
Institute of Childhood
Herzen State Pedagogical University of Russia
Russia
olga_granichina@mail.ru

Elizaveta Tarasova
Saint Petersburg State University
Russia
elizaveta.tarasova@spbu.ru
el.u.tarasova@gmail.com

Article history:
Received 16.04.2026, Accepted 19.06.2026

Abstract

The paper develops a stochastic discrete-time framework for practical fixed-time consensus. Constructive estimates are obtained for the practical consensus set and for the expected entrance time into this set. A comparison-based argument is also established to relate the stochastic dynamics to an ideal noise-free model and to quantify their finite-horizon closeness.

Key words

Multi-agent system, Practical fixed-time consensus, Network load balancing

1 Introduction

Multi-agent systems are extensively employed in robotics, autonomous transportation, sensor networks, and distributed computing. In these applications, each agent typically has access only to local information and can interact directly only with a limited set of neighbor agents. Consequently, achieving a global system-level objective requires the design of distributed coordination mechanisms that ensure the emergence of a prescribed collective behavior across the network. This challenge naturally gives rise to the consensus problem, which has become one of the foundational and most actively studied topics in distributed control theory [Olfati-Saber et al., 2007; Ma et al., 2017].

The role of the communication graph is crucial in such problems, since graph-theoretic characteristics affect qualitative and quantitative properties of distributed algorithms. In this context, Laplacian spectra of basic and hierarchical graphs and their relevance to decentralized optimization and multi-agent control were recently studied in [Erofeeva and Parsegov, 2024].

For standard linear consensus protocols, the closed-loop dynamics typically guarantees only asymptotic convergence. In many engineering applications, however, asymptotic convergence is not sufficient, since one needs an explicit and uniform upper bound on the settling time. This has motivated extensive research on finite-time and fixed-time control based on nonlinear feedback laws and homogeneity arguments. In particular, fixed-time stabilization was systematically developed in [Polyakov, 2012], while fixed-time consensus algorithms for multi-agent systems were studied, for example, in [Parsegov et al., 2013]. At the same time, the passage from continuous-time designs to discrete-time implementations is nontrivial, and consistent discretization of finite-/fixed-time stable systems requires separate analysis [Polyakov et al., 2019; Polyakov et al., 2023].

The stochastic discrete-time setting is substantially more delicate. When agents exchange noisy information over switching communication graphs, exact consensus is generally no longer guaranteed, and the natural objectives become approximate or practical consensus in suitable probabilistic metrics. In this direction, Amelina and Fradkov [Amelina and Fradkov, 2012] investigated approximate consensus in stochastic dynamic networks with incomplete information, measurement delays, and variable topology by means of the local voting protocol and the method of averaged models. This methodology is closely related to the classical continuous-time approximation of discrete stochastic recursive procedures, also known as the Derevitskii–Fradkov–Ljung (DFL) scheme, whose early form goes back to Derevitskii and Fradkov [Derevitskii and Fradkov, 1974]. The local voting approach was further developed for decentralized load balancing over networks with switched topology and noisy measurements in [Amelina, 2013]. In particular, that work considered a discrete-time load-balancing model and introduced a nonlinear local voting protocol that is structurally close to the protocol analyzed in the present paper. A more general approximate-consensus framework for stochastic networks with application to load balancing was proposed in [Amelina et al., 2015], where switching topology, noisy and delayed measurements, and nonvanishing step sizes were considered. Later, Amelina, Granichin, and Kornivetc [Amelina et al., 2013] studied decentralized load balancing under switched topology, noise, and delays, and obtained suboptimality estimates for local voting with nonvanishing step size. Related local-voting mechanisms were also used for distributed node scheduling in multihop wireless networks in [Vergados et al., 2018]. Related distributed resource-allocation problems under communication constraints were also considered in [Fu et al., 2025], where the agents cooperate over a network while exchanging only limited information with their neighbors.

These works justify the importance of local voting protocols in stochastic coordination and load-balancing problems. At the same time, the combination of stochastic discrete-time dynamics, persistent noisy relative measurements, nonlinear mixed-power local voting, and practical fixed-time entrance-time estimates remains less developed.

The relevance of decentralized coordination under noisy and time-varying information structures is also supported by recent studies on adaptive multi-agent systems. For example, decentralized correction of task-time predictions with consensus over a time-varying communication graph and bounded noise was considered in [Tarasova and Moseiko, 2025]. More broadly, recent results on stochastic and discrete-time consensus have mainly addressed mean-square consensus, hybrid or heterogeneous agent dynamics, and delayed or noisy communication [Zhang et al., 2022; Sun et al., 2023; Zhang et al., 2024]. In contrast, constructive practical fixed-time guarantees with explicit entrance-time estimates remain much less developed for stochastic discrete-time multi-agent systems with persistent measurement perturbations.

Another important line of research concerns nonlinear consensus algorithms and finite-time cooperative control based on homogeneity arguments and mixed-power feedback mechanisms. Homogeneity-based methods are useful for constructing fast convergent feedback laws, while implicit Lyapunov-function methods provide an efficient framework for their analysis. Recent works in this direction include finite-time average-consensus constructions and stability analysis for homogeneous systems with sector nonlinearities [Galkina and Zhdanov, 2024; Galkina et al., 2025; Galkina, 2025]. However, most existing finite-/fixed-time consensus results are developed either for deterministic systems or for continuous-time models, whereas the stochastic discrete-time case with persistent measurement perturbations remains much less understood.

This issue is particularly relevant in applications such as decentralized load balancing, where persistent perturbations, nonvanishing gains, and topology variations arise naturally as intrinsic features of the model. In this setting, the appropriate objective is to establish a practical fixed-time consensus guarantee.

In this paper, we study a stochastic discrete-time single-integrator multi-agent system with switching connected communication graphs and a nonlinear local voting protocol. The protocol combines sublinear and superlinear terms, which together induce a Lyapunov drift structure suitable for practical fixed-time analysis.

The main contribution of the paper is the development of a stochastic discrete-time framework for practical fixed-time consensus. We derive constructive estimates for the practical consensus set and the expected entrance time, and establish a comparison-based result relating the stochastic dynamics to an ideal noise-free model. The theoretical findings are further illustrated through a decentralized load-balancing problem.

The remainder of the paper is organized as follows. Section 2 introduces the notation. Section 3 presents the stochastic system, the nonlinear local voting protocol, the comparison model, and the standing assumptions. Section 4 contains the main results, including the mixed-power drift analysis, practical fixed-time consensus estimates, and the finite-horizon trajectory-comparison result. Section 5 presents numerical illustrations. Sections 6 and 7 conclude the paper and outline future research directions, respectively.

2 Notation

Let $\mathbb{R}$ be the set of real numbers, $\mathbb{N}$ the set of positive integers, and $\mathbb{Z}_{\geq 0}$ the set of nonnegative integers. For a vector $x \in \mathbb{R}^n$, $x^\top$ denotes its transpose, x_i its ith component, and $\|x\|$ the Euclidean norm. For a matrix $A \in \mathbb{R}^{n\times n}$, $A^\top$ denotes its transpose, and $\|A\|$ denotes the induced Euclidean norm. The identity matrix of dimension n is denoted by I_n, and $\mathbf{1}_n \in \mathbb{R}^n$ denotes the vector of all ones.

For $s \in \mathbb{R}$ and $\gamma > 0$, define

$$\langle s\rangle^\gamma := |s|^\gamma \operatorname{sign}(s),$$

where $\operatorname{sign}(0) = 0$.

Throughout the paper, capital letters $c, c_1, c_2, \ldots$ denote generic positive constants whose values may change from line to line. Constants introduced in statements of lemmas and theorems are fixed within the corresponding result.

3 Problem statement

3.1 Stochastic System and Practical Consensus

We consider the stochastic discrete-time single-integrator dynamics

$$x_i^{t+1} = x_i^t + u_i^t + w_i^{t+1}, \tag{1}$$

where $i \in \mathcal{N} := \{1, \ldots, n\}$ and $t = 0, 1, 2, \ldots$. Here w_i^t denotes a possible additive state disturbance.

The agents interact according to the nonlinear local voting protocol

$$u_i^t = \alpha \sum_{j=1}^{n} a_{ij}^{(\sigma_t)} \left(K_1 \langle z_{ij}^t \rangle^{1/3} + K_2 \langle z_{ij}^t \rangle^3 \right), \qquad (2)$$

for each $i \in \mathcal{N}$, where

$$z_{ij}^t := x_j^t - x_i^t + \xi_{ij}^t \qquad (3)$$

is the noisy relative state measurement associated with the edge $\{i, j\}$.

The powers $1/3$ and 3 are chosen in accordance with the standard mixed sublinear–superlinear mechanism used in fixed-time stabilization [Polyakov, 2012]. In the Lyapunov analysis below, the term $\langle z \rangle^{1/3}$ generates a drift of order $V^{2/3}$, which is effective near the consensus manifold, whereas the cubic term $\langle z \rangle^3$ generates a drift of order V^2, which provides a contraction mechanism for large disagreements. Other pairs of powers $0 < \gamma_1 < 1 < \gamma_2$, including reciprocal choices such as $1/5$ and 5, are expected to yield analogous mixed-power drift structures. However, they would require a separate proof, with modified constants and, in the stochastic case, different moment requirements on the measurement noise.

Let

$$X_t := [x_1^t, \ldots, x_n^t]^\top, \qquad \Pi := I_n - \frac{1}{n} \mathbf{1}_n \mathbf{1}_n^\top. \qquad (4)$$

Here, X_t is the state vector, Π is the orthogonal projection onto the disagreement subspace, e_t is the disagreement vector, and V_t is the corresponding quadratic disagreement functional. Define

$$e_t := \Pi X_t, \qquad V_t := \frac{1}{2} \|e_t\|^2. \qquad (5)$$

Thus, e_t is the disagreement vector, while V_t is the corresponding Lyapunov function.

Next, introduce the filtration

$$\mathcal{G}_t := \sigma\Big(X_0, \{\sigma_\ell\}_{\ell=0}^{t}, \{\Xi_\ell\}_{\ell=0}^{t-1} \Big), \qquad t \geq 0, \qquad (6)$$

where $\Xi_t = [\xi_{ij}^t]$ is the noise matrix at time t.

Then X_t and σ_t are $\mathcal{G}_t$-measurable, whereas Ξ_t is not. All conditional expectations below are taken with respect to $\mathcal{G}_t$.

For any $\varepsilon > 0$, define the entrance time

$$\tau_\varepsilon := \inf\{t \in \mathbb{Z}_{\geq 0} : V_t \leq \varepsilon\}. \qquad (7)$$

Definition 1. *For a given $\varepsilon > 0$, define the entrance time*

$$\tau_\varepsilon := \inf\{t \in \mathbb{Z}_{\geq 0} : V_t \leq \varepsilon\}.$$

We say that the stochastic discrete-time network achieves semi-global practical fixed-time consensus *on the bounded set $\{V_0 \leq R\}$ if there exist constants $\varepsilon_\star > 0$ and $N_\star > 0$, independent of the particular initial condition inside $\{V_0 \leq R\}$, such that*

$$\mathbb{E}\tau_{\varepsilon_\star} \leq N_\star.$$

Since $\|\Pi X_t\|^2 = 2V_t$, this means that the disagreement enters the practical consensus layer

$$\|\Pi X_t\|^2 \leq 2\varepsilon_\star$$

within an expected time uniformly bounded over all initial conditions satisfying $V_0 \leq R$.

This notion is weaker than classical exact fixed-time consensus: the result concerns entrance into a nonzero practical consensus layer and the uniform bound is imposed on the expected entrance time.

To formalize the trajectory comparison, we introduce the ideal discrete-time system with exact measurements, driven by the same switching graph sequence:

$$\bar{X}_{t+1} = \bar{X}_t + \alpha F_{\sigma_t}(\bar{X}_t), \qquad \bar{X}_0 = X_0. \qquad (8)$$

For each $p \in \{1, \ldots, M\}$, define the mapping $F_p : \mathbb{R}^n \to \mathbb{R}^n$ by

$$[F_p(x)]_i := \sum_{j=1}^{n} a_{ij}^{(p)} \big(K_1 \langle x_j - x_i \rangle^{1/3} + K_2 \langle x_j - x_i \rangle^3 \big), \qquad i \in \mathcal{N}, \qquad (9)$$

where $x = [x_1, \ldots, x_n]^\top \in \mathbb{R}^n$.

The actual stochastic system admits the vector form

$$X^{t+1} = X^t + \alpha G_{\sigma_t}(X^t, \Xi^t) + W^{t+1}, \qquad (10)$$

where $\Xi^t = [\xi_{ij}^t]$ is the matrix of measurement errors and $W^{t+1} = [w_1^{t+1}, \ldots, w_n^{t+1}]^\top$ is the vector of additive state disturbances.

For each $p \in \{1, \ldots, M\}$, define $G_p : \mathbb{R}^n \times \mathbb{R}^{n \times n} \to \mathbb{R}^n$ by

$$[G_p(x, \Xi)]_i := \sum_{j=1}^{n} a_{ij}^{(p)} \big(K_1 \langle x_j - x_i + \xi_{ij} \rangle^{1/3} + K_2 \langle x_j - x_i + \xi_{ij} \rangle^3 \big), \qquad (11)$$

where $i \in \mathcal{N}$.

We compare the disagreement trajectories associated with the stochastic and ideal systems. To this end, define $e_t = \Pi X_t$,, $\bar{e}_t = \Pi \bar{X}_t$.

The corresponding trajectory-comparison error is introduced as

$$\Delta_t := e_t - \bar{e}_t = \Pi(X_t - \bar{X}_t), \qquad D_t := \frac{1}{2} \|\Delta_t\|^2. \qquad (12)$$

We impose the following assumptions.

(H1) **Finite family of undirected connected graphs.** There exists a finite family

$$\mathcal{G} := \{G_p = (\mathcal{N}, E_p, A^{(p)}) : p = 1, \ldots, M\}$$

such that, for every $t \geq 0$, the active communication graph is G_{σ_t} for some $\sigma_t \in \{1, \ldots, M\}$.
Each graph is undirected, connected, and weighted in the sense that

$$a_{ij}^{(p)} = a_{ji}^{(p)} > 0 \quad \text{for } i, j \in E_p,$$

$$a_{ij}^{(p)} = 0 \quad \text{for } i, j \notin E_p, \qquad a_{ii}^{(p)} = 0.$$

Thus, the connectedness assumption refers to the positive-weight edge set E_p.

(H2) **Uniform graph bounds.** The graph family is finite. Hence, the following quantities are well defined and finite:

$$a_{\max} := \max_{p,i,j} a_{ij}^{(p)}, \tag{13}$$

$$\Delta_{\max} := \max_p \max_i \sum_{j=1}^{n} a_{ij}^{(p)}, \tag{14}$$

$$|E|_{\max} := \max_p |E_p|. \tag{15}$$

(H3) **Noisy relative measurements with antisymmetric edge noise.** For each active undirected edge $\{i, j\} \in E_{\sigma_t}$, the random measurement error satisfies

$$\xi_{ij}^t = -\xi_{ji}^t.$$

Assumption (H3) corresponds to a reciprocal edge-measurement model: the same noisy relative measurement is used by the two incident agents with opposite signs. This structure is natural for pairwise exchange and load-balancing protocols. It is also used in the analysis to preserve the average state and to combine the two oriented edge contributions into a dissipative Lyapunov term. Non-antisymmetric directional measurement errors would generate additional perturbation terms; therefore, the present estimates would not apply directly and a separate analysis would be required.

(H4) **Conditional centering and bounded higher moments.** Conditional centering and bounded conditional moments are assumed with respect to the pre-noise filtration. Specifically, for every active edge $\{i, j\} \in E_{\sigma_t}$ and all $t \geq 0$,

$$\mathbb{E}[\xi_{ij}^t \mid \mathcal{G}_t] = 0. \tag{16}$$

Moreover, there exist constants $\mu_2, \mu_4, \mu_6 > 0$ such that, almost surely,

$$\mathbb{E}[|\xi_{ij}^t|^2 \mid \mathcal{G}_t] \leq \mu_2, \tag{17}$$

$$\mathbb{E}[|\xi_{ij}^t|^4 \mid \mathcal{G}_t] \leq \mu_4, \tag{18}$$

$$\mathbb{E}[|\xi_{ij}^t|^6 \mid \mathcal{G}_t] \leq \mu_6, \tag{19}$$

uniformly in i, j, and t.

(H5) **Constant step size.** The gain α is constant and satisfies

$$0 < \alpha \leq 1.$$

(H6) **Bounded initial disagreement.** The initial condition belongs to a prescribed bounded set:

$$V_0 \leq R.$$

(H7) **A priori boundedness/localization of trajectories.** There exists $\widehat{R} \geq R$ such that the sublevel set

$$\Omega_{\widehat{R}} := \left\{ x \in \mathbb{R}^n : \frac{1}{2}\|\Pi x\|^2 \leq \widehat{R} \right\}$$

is forward invariant almost surely for both the actual system (10) and the ideal comparison system (8).
This assumption is not a consequence of the moment bounds in (H4). Rather, it should be understood as a localization condition. It is satisfied under additional boundedness mechanisms, such as bounded measurement errors together with a suitable step-size restriction, or a saturated/projected implementation of the protocol.

(H8) **Parameterized small-noise moment bounds for trajectory comparison.** There exist a scalar $\rho \geq 0$ and constants $\bar{\mu}_2, \bar{\mu}_4, \bar{\mu}_6 > 0$ such that, for every active edge $\{i, j\} \in E_{\sigma_t}$ and all $t \geq 0$, the conditional moments of the measurement noise satisfy, almost surely,

$$\mathbb{E}[|\xi_{ij}^t|^2 \mid \mathcal{G}_t] \leq \rho^2 \bar{\mu}_2, \tag{20}$$

$$\mathbb{E}[|\xi_{ij}^t|^4 \mid \mathcal{G}_t] \leq \rho^4 \bar{\mu}_4, \tag{21}$$

$$\mathbb{E}[|\xi_{ij}^t|^6 \mid \mathcal{G}_t] \leq \rho^6 \bar{\mu}_6. \tag{22}$$

Assumption (H8) refines the moment bounds in (H4) by introducing an explicit noise-level parameter ρ. It is not needed for the practical consensus estimate of Theorem 1, but is used in the finite-horizon comparison with the ideal exact-measurement system, where one needs to quantify the mismatch and prove that it vanishes as $\rho \to 0$.

(H9) **Common initial condition for the comparison system.** The actual and ideal trajectories start from the same initial state:

$$\bar{X}_0 = X_0.$$

Remark on the measurement model. To keep the stochastic discrete-time proof fully self-contained, the main theorems are formulated for current noisy relative measurements on the active edges. The extension to bounded delays can be treated separately as an additional perturbation layer, but it requires an auxiliary estimate and is not needed for the mixed-power homogeneous core of the argument.

4 Main Results

4.1 Homogeneous Edge Functionals

For $r > 0$, define

$$W_r^{(p)}(e) := \sum_{\{i,j\}\in E_p} a_{ij}^{(p)} |e_i - e_j|^r, \tag{23}$$

here $p \in \{1, \dots, M\}$ and $e \in \mathbb{R}^n$. For every $r > 0$, there exist constants $m_r > 0$ and $M_r > 0$ such that

$$m_r\|e\|^r \le W_r^{(p)}(e) \le M_r\|e\|^r \tag{24}$$

for all $e \in \mathbf{1}_n^\perp$ and all $p \in \{1, \dots, M\}$.

By Assumption (H1), the edge set E_p consists of positive-weight edges and is connected.

To justify (24), fix $p \in \{1, \dots, M\}$. The mapping $e \mapsto W_r^{(p)}(e)$ is continuous and positively homogeneous of degree r. Since the graph G_p is connected, the identity $W_r^{(p)}(e) = 0$ with $e \in \mathbf{1}_n^\perp$ implies $e = 0$.

Now consider

$$S := \{e \in \mathbf{1}_n^\perp : \|e\| = 1\}. \tag{25}$$

This set is the unit sphere in the disagreement subspace. Since S is compact, the minimum and maximum of $W_r^{(p)}$ on S are finite. Moreover, both are strictly positive. Taking the minimum and maximum over the finite family of graphs yields uniform constants m_r and M_r.

Lemma 4.1. *Suppose that Assumptions* $(H1)$–$(H5)$ *hold. Then there exist positive constants* c_1, c_2, b_0, b_1, *and* b_2 *such that, for all* $t \ge 0$,

$$\mathbb{E}[V_{t+1} - V_t \mid \mathcal{G}_t] \le -\alpha c_1 V_t^{2/3} - \alpha c_2 V_t^2 + \alpha b_0 + \alpha^2 b_1 V_t^{1/3} + \alpha^2 b_2 V_t^3. \tag{26}$$

The constants c_1, c_2, b_0, b_1, *and* b_2 *depend only on the graph family, the gains* K_1 *and* K_2, *the bounds* μ_2, μ_4, *and* μ_6, *and the graph parameters* $a_{\max}$, $\Delta_{\max}$, *and* $|E|_{\max}$. *In particular, one may take*

$$c_1 = 2^{-1/3} K_1 m_{4/3}, \qquad c_2 = 2K_2 m_4. \tag{27}$$

Proof: For each active undirected edge $\{i, j\} \in E_{\sigma_t}$, define $s_{ij}^t := e_i^t - e_j^t$, $\eta_{ij}^t := -\xi_{ij}^t$, $\zeta_{ij}^t := s_{ij}^t + \eta_{ij}^t$. By Assumption (H3), the edge noise is antisymmetric $\eta_{ji}^t = -\eta_{ij}^t$.

Since the signed-power map is odd, the control satisfies $\mathbf{1}_n^\top u_t = 0$.

Moreover, the analysis is carried out for $W^{t+1} \equiv 0$. Therefore the average state is preserved and

$$e_{t+1} = e_t + u_t.$$

Hence

$$V_{t+1} - V_t = e_t^\top u_t + \frac{1}{2}\|u_t\|^2. \tag{28}$$

Pairing the contributions of the two orientations of each undirected edge, we obtain

$$e_t^\top u_t = -\alpha \sum_{\{i,j\}\in E_{\sigma_t}} a_{ij}^{(\sigma_t)} s_{ij}^t \Big(K_1 \langle \zeta_{ij}^t \rangle^{1/3} + K_2 (\zeta_{ij}^t)^3\Big). \tag{29}$$

For the sublinear contribution,

$$s\langle s+\eta\rangle^{1/3} = |s|^{4/3} + s\Big(\langle s+\eta\rangle^{1/3} - \langle s\rangle^{1/3}\Big).$$

The signed-power map $r \mapsto \langle r\rangle^{1/3}$ is Hölder continuous of order $1/3$, so there exists $C_{1/3} > 0$ such that

$$\big|\langle s+\eta\rangle^{1/3} - \langle s\rangle^{1/3}\big| \le C_{1/3}|\eta|^{1/3}.$$

Consequently,

$$s\langle s+\eta\rangle^{1/3} \ge |s|^{4/3} - C_{1/3}|s|\,|\eta|^{1/3}.$$

Applying Young's inequality with conjugate exponents $4/3$ and 4, we obtain

$$|s|\,|\eta|^{1/3} \le \frac{1}{2C_{1/3}}|s|^{4/3} + \widetilde{C}_{1/3}|\eta|^{4/3},$$

Therefore, we can say that

$$s\langle s+\eta\rangle^{1/3} \ge \frac{1}{2}|s|^{4/3} - \widehat{C}_{1/3}|\eta|^{4/3}. \tag{30}$$

For the cubic term, expand

$$s(s+\eta)^3 = s^4 + 3s^3\eta + 3s^2\eta^2 + s\eta^3.$$

Using Young's inequality on each mixed term, there exists a constant $\widehat{C}_3 > 0$ such that

$$s(s+\eta)^3 \ge \frac{1}{2}s^4 - \widehat{C}_3|\eta|^4. \tag{31}$$

Substituting (30) and (31) into (29), we obtain

$$
\begin{aligned}
e_t^\top u_t \le & -\frac{\alpha K_1}{2}\sum_{\{i,j\}\in E_{\sigma_t}} a_{ij}^{(\sigma_t)}|s_{ij}^t|^{4/3} \\
& -\frac{\alpha K_2}{2}\sum_{\{i,j\}\in E_{\sigma_t}} a_{ij}^{(\sigma_t)}|s_{ij}^t|^{4} \\
& +\alpha C_0\sum_{\{i,j\}\in E_{\sigma_t}} a_{ij}^{(\sigma_t)}\big(|\eta_{ij}^t|^{4/3}+|\eta_{ij}^t|^4\big),
\end{aligned} \tag{32}
$$

for some constant $C_0 > 0$.

Using the homogeneous norm equivalence on $\mathbf{1}_n^\perp$, we obtain

$$\sum_{\{i,j\}\in E_{\sigma_t}} a_{ij}^{(\sigma_t)}|s_{ij}^t|^{4/3} = W_{4/3}^{(\sigma_t)}(e_t) \ge m_{4/3}(2V_t)^{2/3},$$

and

$$\sum_{\{i,j\}\in E_{\sigma_t}} a_{ij}^{(\sigma_t)}|s_{ij}^t|^{4} = W_{4}^{(\sigma_t)}(e_t) \ge 4m_4 V_t^2.$$

Taking conditional expectations in (32) and using Assumption (H4) together with Jensen's inequality $\mathbb{E}[|\eta|^{4/3} \mid \mathcal{G}_t] \le \mu_2^{2/3}$, we obtain

$$\mathbb{E}[e_t^\top u_t \mid \mathcal{G}_t] \le -\alpha c_1 V_t^{2/3} - \alpha c_2 V_t^2 + \alpha\beta_0, \tag{33}$$

where

$$c_1 := 2^{-1/3}K_1 m_{4/3}, \qquad c_2 := 2K_2 m_4,$$

and $\beta_0 > 0$ depends only on $C_0, a_{\max}, |E|_{\max}, \mu_2, \mu_4$.

By the definition of the protocol, Cauchy–Schwarz inequality, and $(r+s)^2 \le 2r^2 + 2s^2$,

$$
\begin{aligned}
\|u_t\|^2 &= \sum_{i=1}^n \left|\alpha \sum_{j=1}^n a_{ij}^{(\sigma_t)}\Big(K_1|\zeta_{ij}^t|^{1/3} + K_2|\zeta_{ij}^t|^3\Big)\operatorname{sign}(\zeta_{ij}^t)\right|^2 \\
&\le \alpha^2\Delta_{\max}\sum_{i=1}^n\sum_{j=1}^n a_{ij}^{(\sigma_t)}\Big(K_1|\zeta_{ij}^t|^{1/3} + K_2|\zeta_{ij}^t|^3\Big)^2 \\
&\le 2\alpha^2\Delta_{\max}\sum_{i=1}^n\sum_{j=1}^n a_{ij}^{(\sigma_t)}\Big(K_1^2|\zeta_{ij}^t|^{2/3} + K_2^2|\zeta_{ij}^t|^6\Big).
\end{aligned}
$$

Since

$$|r+s|^{2/3} \le 2^{2/3}\big(|r|^{2/3}+|s|^{2/3}\big), \tag{34}$$

and

$$|r+s|^6 \le 32\big(|r|^6+|s|^6\big), \tag{35}$$

there exists a constant $C_1 > 0$ such that

$$
\begin{aligned}
\|u_t\|^2 \le\, & \alpha^2 C_1 \sum_{\{i,j\}\in E_{\sigma_t}} a_{ij}^{(\sigma_t)}|s_{ij}^t|^{2/3} \\
& + \alpha^2 C_1 \sum_{\{i,j\}\in E_{\sigma_t}} a_{ij}^{(\sigma_t)}|s_{ij}^t|^{6} \\
& + \alpha^2 C_1 \sum_{\{i,j\}\in E_{\sigma_t}} a_{ij}^{(\sigma_t)}|\eta_{ij}^t|^{2/3} \\
& + \alpha^2 C_1 \sum_{\{i,j\}\in E_{\sigma_t}} a_{ij}^{(\sigma_t)}|\eta_{ij}^t|^{6}.
\end{aligned} \tag{36}
$$

Next, observe that

$$\|e_t\|^{2/3} = (2V_t)^{1/3}, \tag{37}$$

and

$$\|e_t\|^6 = (2V_t)^3 = 8V_t^3. \tag{38}$$

Using the upper homogeneous norm equivalence, we obtain

$$\sum_{\{i,j\}\in E_{\sigma_t}} a_{ij}^{(\sigma_t)}|s_{ij}^t|^{2/3} \le M_{2/3}(2V_t)^{1/3}, \tag{39}$$

and

$$\sum_{\{i,j\}\in E_{\sigma_t}} a_{ij}^{(\sigma_t)}|s_{ij}^t|^{6} \le 8M_6 V_t^3. \tag{40}$$

Taking conditional expectations and using

$$\mathbb{E}[|\eta_{ij}^t|^{2/3} \mid \mathcal{G}_t] \le \mu_2^{1/3}, \qquad \mathbb{E}[|\eta_{ij}^t|^{6} \mid \mathcal{G}_t] \le \mu_6,$$

we arrive at

$$\mathbb{E}[\|u_t\|^2 \mid \mathcal{G}_t] \le \alpha^2\left(d_0 + d_1 V_t^{1/3} + d_2 V_t^3\right), \tag{41}$$

for some positive constants d_0, d_1, d_2 depending only on the graph family, the gains, and the moment bounds.

Substituting (33) and (41) into (28), we obtain

$$
\begin{aligned}
\mathbb{E}[V_{t+1} - V_t \mid \mathcal{G}_t] \le & -\alpha c_1 V_t^{2/3} - \alpha c_2 V_t^2 + \alpha\beta_0 \\
& + \frac{\alpha^2}{2}\big(d_0 + d_1 V_t^{1/3} + d_2 V_t^3\big).
\end{aligned} \tag{42}
$$

Since $\alpha \in (0,1]$ by Assumption (H5), it follows that

$$\frac{\alpha^2 d_0}{2} \le \frac{\alpha d_0}{2}. \tag{43}$$

Now define

$$b_0 := \beta_0 + \frac{d_0}{2}, \qquad b_1 := \frac{d_1}{2}, \qquad b_2 := \frac{d_2}{2}. \tag{44}$$

Here b_0, b_1, and b_2 are the constants appearing in (26). With these definitions, inequality (26). follows. This completes the proof.

Remark. The signed-power terms of orders $1/3$ and 3 generate two different homogeneous drift mechanisms. The term $\langle s\rangle^{1/3}$ produces a drift proportional to $V^{2/3}$ and is therefore responsible for the fast approach to the consensus layer near the origin. The term $\langle s\rangle^3$ produces a drift proportional to V^2 and provides a uniform contraction mechanism for large disagreements.

4.2 Practical Fixed-Time Consensus

Theorem 1. *Suppose that Assumptions* (H1)–(H7) *hold. Let* $c_1, c_2, b_0, b_1, b_2 > 0$ *be the constants from Lemma 4.1. Assume, that*

$$\alpha b_2 \widehat{R} \le \frac{c_2}{2}, \tag{45}$$

and

$$\varepsilon_\star := \max\left\{\left(\frac{2b_0}{c_1}\right)^{3/2}, \left(\frac{2\alpha b_1}{c_1}\right)^3\right\} < 1. \tag{46}$$

Then, for every initial condition such that $V_0 \le R$*, the entrance time*

$$\tau_{\varepsilon_\star} := \inf\{t \ge 0 :\ V_t \le \varepsilon_\star\} \tag{47}$$

satisfies

$$\mathbb{E}\tau_{\varepsilon_\star} \le N_\star, \tag{48}$$

where

$$N_\star := \left\lceil \frac{6}{\alpha c_1} + \frac{2}{\alpha c_2} \right\rceil. \tag{49}$$

Consequently,

$$\mathbb{E}\|\Pi X_{\tau_{\varepsilon_\star}}\|^2 \le 2\varepsilon_\star. \tag{50}$$

That is, the stochastic discrete-time protocol achieves semi-global practical fixed-time consensus on the bounded set $\{V_0 \le R\}$.

Proof. By Lemma 4.1

$$\mathbb{E}[V_{t+1} - V_t \mid \mathcal{G}_t] \le -\alpha c_1 V_t^{2/3} - \alpha c_2 V_t^2 + \alpha b_0 + \alpha^2 b_1 V_t^{1/3} + \alpha^2 b_2 V_t^3. \tag{51}$$

By Assumption (H7), one has $V_t \le \widehat{R}$ almost surely for all $t \ge 0$. Therefore,

$$\begin{aligned}\alpha^2 b_2 V_t^3 &= \alpha^2 b_2 V_t\, V_t^2 \\ &\le \alpha^2 b_2 \widehat{R}\, V_t^2 \\ &\le \frac{\alpha c_2}{2} V_t^2.\end{aligned} \tag{52}$$

Next, suppose that $V_t \ge \varepsilon_\star$. Then, by (46),

$$\alpha b_0 \le \frac{\alpha c_1}{2} V_t^{2/3}, \tag{53}$$

and

$$\alpha^2 b_1 V_t^{1/3} \le \frac{\alpha c_1}{2} V_t^{2/3}. \tag{54}$$

Hence, for all t such that $V_t \in [\varepsilon_\star, \widehat{R}]$,

$$\mathbb{E}[V_{t+1} - V_t \mid \mathcal{G}_t] \le -\frac{\alpha c_1}{2} V_t^{2/3} - \frac{\alpha c_2}{2} V_t^2. \tag{55}$$

Define

$$\tau_\star := \tau_{\varepsilon_\star} = \inf\{t \ge 0 : V_t \le \varepsilon_\star\}, \qquad Y_t := V_{t\wedge\tau_\star}.$$

Set

$$g(s) := \frac{c_1}{2} s^{2/3} + \frac{c_2}{2} s^2, \qquad s > 0.$$

Consider the function

$$\Phi(s) := \begin{cases} \dfrac{s}{g(\varepsilon_\star)}, & 0 \le s \le \varepsilon_\star, \\ \dfrac{\varepsilon_\star}{g(\varepsilon_\star)} + \displaystyle\int_{\varepsilon_\star}^{s} \frac{dr}{g(r)}, & s > \varepsilon_\star. \end{cases}$$

The function Φ is nonnegative and concave on $[0,\infty)$. Moreover, for $s > \varepsilon_\star$,

$$\Phi'(s) = \frac{1}{g(s)}.$$

On the event $\{t < \tau_\star\}$, one has $V_t > \varepsilon_\star$. By (55),

$$\mathbb{E}[V_{t+1} - V_t \mid \mathcal{G}_t] \le -\alpha g(V_t).$$

Using the concavity of Φ, we obtain on the event $\{t < \tau_\star\}$

$$\Phi(V_{t+1}) - \Phi(V_t) \le \Phi'(V_t)(V_{t+1} - V_t).$$

Since $Y_t = V_t$ and $Y_{t+1} = V_{t+1}$ on the event $\{t < \tau_\star\}$, whereas $Y_{t+1} = Y_t$ on the event $\{t \ge \tau_\star\}$, and since $\{t < \tau_\star\} \in \mathcal{G}_t$, we get

$$\mathbb{E}[\Phi(Y_{t+1}) - \Phi(Y_t) \mid \mathcal{G}_t] \le -\alpha \mathbf{1}_{\{t<\tau_\star\}}.$$

Taking expectations and summing from $t = 0$ to $N-1$, we obtain

$$\mathbb{E}\Phi(Y_N) - \mathbb{E}\Phi(Y_0) \le -\alpha \sum_{t=0}^{N-1} \mathbb{P}(t < \tau_\star).$$

Since $\Phi \geq 0$, it follows that

$$\alpha\,\mathbb{E}(N \wedge \tau_\star) \leq \mathbb{E}\Phi(Y_0).$$

Since $\varepsilon_\star < 1$, for all $s \geq 0$ we have

$$\Phi(s) \leq \frac{\varepsilon_\star}{g(\varepsilon_\star)} + \int_{\varepsilon_\star}^{1} \frac{2\,dr}{c_1 r^{2/3}} + \int_{1}^{\infty} \frac{2\,dr}{c_2 r^2}.$$

Therefore,

$$\mathbb{E}\Phi(Y_0) \leq \frac{\varepsilon_\star}{g(\varepsilon_\star)} + \int_{\varepsilon_\star}^{1} \frac{2\,dr}{c_1 r^{2/3}} + \int_{1}^{\infty} \frac{2\,dr}{c_2 r^2}.$$

Hence,

$$\mathbb{E}\Phi(Y_0) \leq \frac{2\varepsilon_\star^{1/3}}{c_1} + \frac{6(1-\varepsilon_\star^{1/3})}{c_1} + \frac{2}{c_2} \leq \frac{6}{c_1} + \frac{2}{c_2}.$$

Letting $N \to \infty$ and using monotone convergence, we obtain

$$\mathbb{E}\tau_{\varepsilon_\star} \leq \frac{6}{\alpha c_1} + \frac{2}{\alpha c_2}.$$

Taking the ceiling gives (49).

Since $V_{\tau_{\varepsilon_\star}} \leq \varepsilon_\star$ almost surely and $\|\Pi X_t\|^2 = 2V_t$, we obtain (50).

The theorem is proved.

4.3 Finite-Horizon Trajectory Comparison

Lemma 4.2. *Suppose that Assumptions* (H1)–(H9) *hold. Then there exist positive constants L_1, L_2, and M_0 such that, for every $p \in \{1,\ldots,M\}$, the following estimates hold.*

The constants L_1, L_2, and M_0 depend only on R_b, the graph family, and the gains K_1 and K_2.

(i) For all $x, z \in \Omega_{R_b}$,

$$\|F_p(x)-F_p(z)\| \leq L_1\|\Pi(x-z)\|^{1/3} + L_2\|\Pi(x-z)\|. \tag{56}$$

(ii) For all $x \in \Omega_{R_b}$ and all $t \geq 0$,

$$\mathbb{E}\big[\|G_{\sigma_t}(x,\Xi_t) - F_{\sigma_t}(x)\|^2 \,\big|\, \mathcal{G}_t\big] \leq M_0\, q_\rho, \tag{57}$$

where

$$q_\rho := \rho^{2/3} + \rho^{4/3} + \rho^2 + \rho^4 + \rho^6. \tag{58}$$

Proof. Fix $p \in \{1,\ldots,M\}$.

For part (i), define for each oriented edge (i,j),

$$s_{ij}(x) := x_j - x_i, \qquad s_{ij}(z) := z_j - z_i.$$

Since the signed-power map $r \mapsto \langle r\rangle^{1/3}$ is globally Hölder continuous of order $1/3$, there exists $C_H > 0$ such that

$$\big|\langle s_{ij}(x)\rangle^{1/3} - \langle s_{ij}(z)\rangle^{1/3}\big| \leq C_H|s_{ij}(x) - s_{ij}(z)|^{1/3}. \tag{59}$$

Since Ω_{R_b} is bounded, all edge differences are uniformly bounded on Ω_{R_b}. Hence the cubic signed power map is Lipschitz on the corresponding compact interval.

Therefore, there exists $C_3 > 0$ such that

$$\big|\langle s_{ij}(x)\rangle^{3} - \langle s_{ij}(z)\rangle^{3}\big| \leq C_3|s_{ij}(x) - s_{ij}(z)|. \tag{60}$$

Thus, for every i,

$$\begin{aligned} |[F_p(x) - F_p(z)]_i| \leq{}& K_1 C_H \sum_{j=1}^{n} a_{ij}^{(p)} \\ &\times \big|(x_j - z_j) - (x_i - z_i)\big|^{1/3} \\ &+ K_2 C_3 \sum_{j=1}^{n} a_{ij}^{(p)} \\ &\times \big|(x_j - z_j) - (x_i - z_i)\big|. \end{aligned} \tag{61}$$

Now apply the finiteness of the graph family, the uniform degree bound, and norm equivalence on $\mathbf{1}_n^{\perp}$. This yields (56).

Define

$$\begin{aligned} r_{ij}(x,\Xi) :={}& K_1\Big(\langle x_j - x_i + \xi_{ij}\rangle^{1/3} - \langle x_j - x_i\rangle^{1/3}\Big) \\ &+ K_2\Big(\langle x_j - x_i + \xi_{ij}\rangle^{3} - \langle x_j - x_i\rangle^{3}\Big). \end{aligned} \tag{62}$$

Here $r_{ij}(x,\Xi)$ denotes the edgewise perturbation induced by the measurement error ξ_{ij}.

By the same Hölder and local Lipschitz estimates, there exist constants $C_1, C_2 > 0$, depending only on R_b, K_1, and K_2, such that

$$|r_{ij}(x,\Xi)| \leq C_1|\xi_{ij}|^{1/3} + C_2|\xi_{ij}| + C_2|\xi_{ij}|^3. \tag{63}$$

Let $y_{ij} := |\xi_{ij}|$. Squaring (63) and using Young's inequality for the mixed products, we obtain, with a possibly larger constant $C > 0$,

$$|r_{ij}(x,\Xi)|^2 \leq C\left(y_{ij}^{2/3} + y_{ij}^{4/3} + y_{ij}^{2} + y_{ij}^{10/3} + y_{ij}^{4} + y_{ij}^{6}\right).$$

Since, for all $y \geq 0$,

$$y^{10/3} \leq y^2 + y^4,$$

the term of order $10/3$ is absorbed into the terms of orders 2 and 4.

Therefore, for some constant $C > 0$,

$$
\begin{aligned}
\|G_p(x,\Xi)-F_p(x)\|^2 \le C &\sum_{\{i,j\}\in E_p} a_{ij}^{(p)}|\xi_{ij}|^{2/3}\\
&+C\sum_{\{i,j\}\in E_p} a_{ij}^{(p)}|\xi_{ij}|^{4/3}\\
&+C\sum_{\{i,j\}\in E_p} a_{ij}^{(p)}|\xi_{ij}|^{2}\\
&+C\sum_{\{i,j\}\in E_p} a_{ij}^{(p)}|\xi_{ij}|^{4}\\
&+C\sum_{\{i,j\}\in E_p} a_{ij}^{(p)}|\xi_{ij}|^{6}.
\end{aligned} \tag{64}
$$

The constant C depends only on the graph family and the gains.

Next, take conditional expectations with respect to $\mathcal{G}_t$. Using Assumption (H8) together with Jensen's inequality, we obtain

$$
\begin{aligned}
&\mathbb{E}\big[\,\|G_{\sigma_t}(x,\Xi_t)-F_{\sigma_t}(x)\|^2 \,\big|\, \mathcal{G}_t\big]\\
&\qquad\le M_0\big(\rho^{2/3}+\rho^{4/3}+\rho^2+\rho^4+\rho^6\big).
\end{aligned} \tag{65}
$$

Finally, define

$$
q_\rho := \rho^{2/3}+\rho^{4/3}+\rho^2+\rho^4+\rho^6. \tag{66}
$$

Then (65) takes the form

$$
\mathbb{E}\big[\|G_{\sigma_t}(x,\Xi_t)-F_{\sigma_t}(x)\|^2 \,\big|\, \mathcal{G}_t\big] \le M_0 q_\rho. \tag{67}
$$

This proves (67).

Theorem 2. *Suppose that Assumptions* (H1)–(H9) *hold. Define*

$$
\Delta_t := \Pi(X_t-\bar{X}_t), \tag{68}
$$

and

$$
D_t := \frac{1}{2}\|\Delta_t\|^2, d_t := \mathbb{E}D_t. \tag{69}
$$

Here Δ_t is the projected trajectory-comparison error, D_t is its quadratic measure, and d_t is its expectation.

Let L_1, L_2, and M_0 be the constants from Lemma 4.2. Next, define

$$
a_0 := 2^{4/3}L_1^2, \tag{70}
$$

$$
a_1 := 2^{2/3}L_1, \tag{71}
$$

$$
a_2 := 1+2L_2+4L_2^2, \tag{72}
$$

and

$$
a_3 := \frac{3}{2}M_0. \tag{73}
$$

Then, for every $t \ge 0$,

$$
\begin{aligned}
d_{t+1} \le d_t + \alpha a_0 d_t^{1/3} + \alpha a_1 d_t^{2/3}&\\
+\alpha a_2 d_t + \alpha a_3 q_\rho&.
\end{aligned} \tag{74}
$$

Consequently, if the scalar sequence $\{z_t\}_{t\ge0}$ is defined by

$$
\begin{aligned}
&z_0 = 0,\\
&z_{t+1} = z_t + \alpha\Big(a_0 z_t^{1/3} + a_1 z_t^{2/3} + a_2 z_t + a_3 q_\rho\Big),
\end{aligned} \tag{75}
$$

then

$$
d_t \le z_t, \qquad \forall t \ge 0. \tag{76}
$$

In particular, for every fixed $N \in \mathbb{N}$,

$$
\sup_{0\le t\le N} \mathbb{E}\|\Pi(X_t-\bar{X}_t)\|^2 = 2\sup_{0\le t\le N} d_t \le 2z_N. \tag{77}
$$

Moreover, for every fixed N,

$$
z_N \to 0 \qquad \text{as} \qquad \rho \to 0.
$$

Hence the disagreement trajectories of the stochastic system and the ideal exact-measurement system are uniformly close in mean square on every fixed finite horizon, and the closeness radius vanishes with the noise level.

Proof. Using the reduced form of the actual system with $W^{t+1} \equiv 0$, it follows from (10) and (8) that

$$
\Delta_{t+1} = \Delta_t + \alpha A_t + \alpha B_t, \tag{78}
$$

where

$$
A_t := \Pi\big(F_{\sigma_t}(X_t) - F_{\sigma_t}(\bar{X}_t)\big), \tag{79}
$$

and

$$
B_t := \Pi\big(G_{\sigma_t}(X_t,\Xi_t) - F_{\sigma_t}(X_t)\big). \tag{80}
$$

Here A_t is the deterministic increment mismatch, whereas B_t is the noise-induced increment error.

Since both F_{σ_t} and G_{σ_t} preserve the average on undirected graphs with antisymmetric edge perturbations, the projector Π may be omitted in the corresponding norm estimates. Therefore,

$$D_{t+1} - D_t = \alpha \Delta_t^\top A_t + \alpha \Delta_t^\top B_t + \frac{\alpha^2}{2} \|A_t + B_t\|^2. \tag{81}$$

By Lemma 4.2,

$$\|A_t\| \le L_1 \|\Delta_t\|^{1/3} + L_2 \|\Delta_t\|.$$

Hence

$$|\Delta_t^\top A_t| \le \|\Delta_t\| \, \|A_t\| \le L_1 \|\Delta_t\|^{4/3} + L_2 \|\Delta_t\|^2.$$

Since $\|\Delta_t\|^2 = 2D_t$, this implies

$$|\Delta_t^\top A_t| \le c_1 D_t^{2/3} + c_2 D_t \tag{82}$$

for suitable positive constants c_1, c_2.

Next, apply Young's inequality together with Lemma 4.2. This yields

$$\mathbb{E}\big[|\Delta_t^\top B_t| \mid \mathcal{G}_t\big] \le \frac{1}{2} \|\Delta_t\|^2 + \frac{1}{2} \mathbb{E}[\|B_t\|^2 \mid \mathcal{G}_t]. \tag{83}$$

Since $D_t = \frac{1}{2}\|\Delta_t\|^2$, and by Lemma 4.2,

$$\mathbb{E}\big[|\Delta_t^\top B_t| \mid \mathcal{G}_t\big] \le D_t + \frac{M_0}{2} q_\rho. \tag{84}$$

Therefore,

$$\mathbb{E}\big[\alpha \Delta_t^\top B_t \mid \mathcal{G}_t\big] \le \alpha D_t + \frac{\alpha M_0}{2} q_\rho. \tag{85}$$

For the quadratic term, we use the elementary inequality

$$(u+v)^2 \le 2u^2 + 2v^2. \tag{86}$$

Hence,

$$\|A_t + B_t\|^2 \le 2\|A_t\|^2 + 2\|B_t\|^2. \tag{87}$$

Next, by Lemma 4.2,

$$\|A_t\|^2 \le 2L_1^2 \|\Delta_t\|^{2/3} + 2L_2^2 \|\Delta_t\|^2. \tag{88}$$

Using $D_t = \frac{1}{2}\|\Delta_t\|^2$, we obtain

$$\|A_t\|^2 \le \widetilde{c}_1 D_t^{1/3} + \widetilde{c}_2 D_t, \tag{89}$$

where

$$\widetilde{c}_1 := 2^{4/3} L_1^2, \qquad \widetilde{c}_2 := 4L_2^2. \tag{90}$$

Therefore

$$\frac{\alpha^2}{2} \mathbb{E}[\|A_t + B_t\|^2 \mid \mathcal{G}_t] \le \alpha^2 \widetilde{c}_1 D_t^{1/3} + \alpha^2 \widetilde{c}_2 D_t + \alpha^2 M_0 q_\rho. \tag{91}$$

Since $0 < \alpha \le 1$, it follows that $\alpha^2 \le \alpha$. Hence,

$$\frac{\alpha^2}{2} \mathbb{E}[\|A_t + B_t\|^2 \mid \mathcal{G}_t] \le \alpha \widetilde{c}_1 D_t^{1/3} + \alpha \widetilde{c}_2 D_t + \alpha M_0 q_\rho. \tag{92}$$

Substituting (82), (85), and (92) into (81), we obtain

$$\mathbb{E}[D_{t+1} - D_t \mid \mathcal{G}_t] \le \alpha \Big(a_0 D_t^{1/3} + a_1 D_t^{2/3} + a_2 D_t + a_3 q_\rho \Big)$$

for suitable positive constants a_0, a_1, a_2, a_3.

Taking expectations and using Jensen's inequality for the concave functions $s \mapsto s^{1/3}$ and $s \mapsto s^{2/3}$ gives

$$d_{t+1} \le d_t + \alpha \Big(a_0 d_t^{1/3} + a_1 d_t^{2/3} + a_2 d_t + a_3 q_\rho \Big),$$

which is exactly (74).

Now define z_t by (75). Since $d_0 = D_0 = 0 = z_0$ and the right-hand side of (75) is monotone increasing in z_t, a straightforward induction yields $d_t \le z_t$ for all $t \ge 0$.

Finally,

$$\mathbb{E}\|\Pi(X_t - \bar{X}_t)\|^2 = 2d_t \le 2z_t \le 2z_N, \qquad 0 \le t \le N.$$

For fixed N, the recursion (75) depends continuously on q_ρ, and when $\rho = 0$ one has $q_\rho = 0$ and $z_t \equiv 0$.

Therefore $z_N \to 0$ as $\rho \to 0$. The theorem is proved.

4.4 Transfer of practical convergence from the ideal trajectory

Under the assumptions of Theorem 2, let

$$\bar{e}_t := \Pi \bar{X}_t, \qquad \bar{V}_t := \frac{1}{2}\|\bar{e}_t\|^2.$$

Then, for every $t \ge 0$,

$$\mathbb{E} V_t \le 2\,\mathbb{E} \bar{V}_t + 2z_t. \tag{93}$$

Consequently, if for some $N \in \mathbb{N}$,

$$\mathbb{E} \bar{V}_N \le \bar{\varepsilon}, \tag{94}$$

then the actual stochastic trajectory satisfies

$$\mathbb{E} V_N \le 2\bar{\varepsilon} + 2z_N. \tag{95}$$

Equivalently,

$$\mathbb{E}\|\Pi X_N\|^2 \le 4\bar{\varepsilon} + 4z_N. \tag{96}$$

If, in particular, $\bar{V}_N \le \bar{\varepsilon}$ almost surely (for example, when the switching sequence is deterministic), then (95)–(96) follow immediately as a special case.

Proof. Since

$$e_t = \bar{e}_t + \Delta_t,$$

we have

$$V_t = \frac{1}{2}\|e_t\|^2 = \frac{1}{2}\|\bar{e}_t+\Delta_t\|^2 \le \|\bar{e}_t\|^2+\|\Delta_t\|^2 = 2\bar{V}_t+2D_t.$$

Taking expectations and using Theorem 2, we obtain

$$\mathbb{E}V_t \le 2\,\mathbb{E}\bar{V}_t + 2\,\mathbb{E}D_t = 2\,\mathbb{E}\bar{V}_t + 2d_t \le 2\,\mathbb{E}\bar{V}_t + 2z_t.$$

This proves (93). Setting $t = N$ and using (94) yields (95).

Multiplying by 2 gives (96).

5 Experiments

This section provides a numerical illustration of the theoretical results for a stochastic discrete-time multi-agent system over a switching communication network. The purpose of the simulations is threefold: first, to demonstrate the decay of the disagreement energy toward a small practical neighborhood of the consensus manifold; second, to illustrate the role of the two mixed-power terms in the proposed local voting protocol; third, to illustrate the finite-horizon mean-square closeness between the actual stochastic trajectory and the corresponding ideal exact-measurement trajectory.

We consider a network of $n = 8$ agents with single-integrator dynamics and the nonlinear local voting protocol introduced above. The communication topology switches periodically between the two sparse connected undirected graphs shown in Fig. 1. The first graph is the path

$$E_1 = \{(1,2),(2,3),(3,4),(4,5),\\ (5,6),(6,7),(7,8)\},$$

whereas the second graph is the sparse connected tree

$$E_2 = \{(1,4),(4,2),(2,6),(6,3),\\ (3,8),(8,5),(5,7)\}.$$

Both graphs have $n-1 = 7$ edges and diameter 7. The switching law is given by

$$\sigma_t = \begin{cases} 1, & \text{if } t \text{ is even,} \\ 2, & \text{if } t \text{ is odd.} \end{cases}$$

The initial states are chosen as

$$x_1^0 = 5.5, \quad x_2^0 = 3.5, \quad x_3^0 = 2.3, \quad x_4^0 = 3.15,$$

$$x_5^0 = 7.4, \quad x_6^0 = 1.1, \quad x_7^0 = 2.8, \quad x_8^0 = 9.9.$$

For this initial condition, the average value is

$$\bar{x} = \frac{1}{n}\sum_{i=1}^{n} x_i^0 = 4.45625,$$

and the initial disagreement energy is

$$V_0 = \frac{1}{2}\|\Pi X_0\|^2 \approx 30.3336.$$

The measurement noise is generated explicitly as follows. For each Monte Carlo run, each time instant t, and each active undirected edge $\{i,j\} \in E_{\sigma_t}$, we independently generate

$$\omega_{ij}^t \sim \mathcal{U}[-1,1]$$

and set

$$\xi_{ij}^t = \rho\,\omega_{ij}^t, \qquad \xi_{ji}^t = -\xi_{ij}^t.$$

For inactive edges, the corresponding measurement error is set to zero. Thus, the simulated noise is zero-mean, bounded, and antisymmetric on each active edge. Moreover,

$$\mathbb{E}|\xi_{ij}^t|^2 = \frac{\rho^2}{3}, \quad \mathbb{E}|\xi_{ij}^t|^4 = \frac{\rho^4}{5}, \quad \mathbb{E}|\xi_{ij}^t|^6 = \frac{\rho^6}{7},$$

which is consistent with Assumptions (H3), (H4), and (H8).

The reported empirical characteristics are computed over $N_{\mathrm{MC}} = 200$ Monte Carlo runs on the horizon $T = 140$. In all numerical experiments, the additive state disturbance in (1) is set to zero, $w_i^{t+1} \equiv 0$, consistently with the theoretical analysis. The step size is fixed at $\alpha = 0.04$. In the practical-consensus and ablation experiments, the noise amplitude is $\rho = 0.10$. In the trajectory-comparison experiment, the same switching law and initial condition are used while the noise amplitude is varied over $\rho \in \{0.03, 0.07, 0.12\}$. The base random seed is fixed at 12345. Common random numbers are used across gain pairs, ablation protocols, and noise amplitudes in order to make the comparisons reproducible.

To characterize the consensus behaviour, we use the disagreement energy

$$V_t = \frac{1}{2}\|\Pi X_t\|^2.$$

For the comparison experiment, we also simulate the ideal exact-measurement system driven by the same switching sequence and compute

$$D_t = \frac{1}{2}\|\Pi(X_t - \bar{X}_t)\|^2.$$

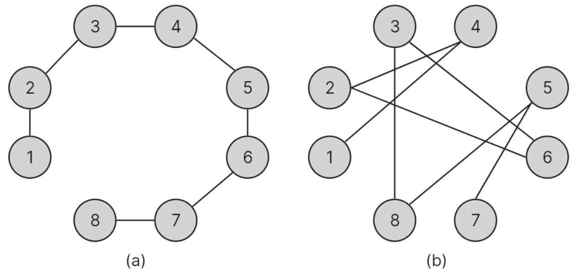

Figure 1. Two sparse connected switching communication graphs used in the simulations.

Practical Consensus Behaviour We first examine the disagreement decay for several gain pairs (K_1, K_2). For each choice of gains, we compute the empirical disagreement

$$\widehat{V}_t := \frac{1}{N_{\mathrm{MC}}} \sum_{k=1}^{N_{\mathrm{MC}}} V_t^{(k)},$$

where $V_t^{(k)}$ is the disagreement energy in the k-th run. The corresponding results are shown in Fig. 2.

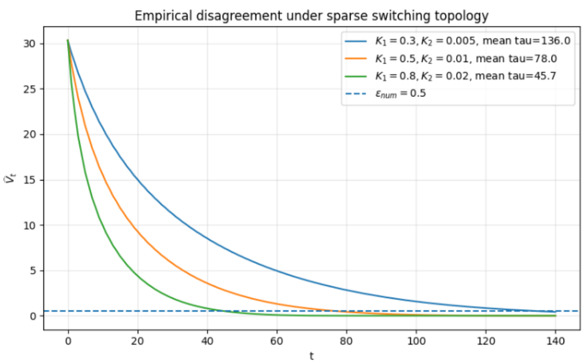

Figure 2. Empirical disagreement $\widehat{V}_t$ for three gain pairs (K_1, K_2), averaged over $N_{\mathrm{MC}} = 200$ runs. The dashed line indicates the numerical practical layer $\varepsilon_{\mathrm{num}} = 0.5$. The shaded regions indicate empirical 5–95 percentile ranges.

The figure shows a clear decay of $\widehat{V}_t$ toward a small practical neighborhood of the consensus manifold. Larger values of K_1 and K_2 shorten the transient stage and lead to a faster decrease of the empirical disagreement, which is consistent with the mixed-power drift mechanism established in Section 4. The dashed horizontal line in Fig. 2 indicates a numerical practical layer $\varepsilon_{\mathrm{num}} = 0.5$, used only for visualization of the entrance behaviour and not intended to coincide with the conservative theoretical value $\varepsilon_\star$.

To quantify the transient stage, we define the empirical entrance time

$$\widehat{\tau}^{(k)}_{\varepsilon_{\mathrm{num}}} := \inf\{0 \le t \le T : \; V_t^{(k)} \le \varepsilon_{\mathrm{num}}\}.$$

If the layer is not reached by time T, we set $\widehat{\tau}^{(k)}_{\varepsilon_{\mathrm{num}}} = T + 1$. For the gain pairs shown in Fig. 2, the corresponding empirical mean entrance times are approximately

$$\widehat{\mathbb{E}}\tau_{\varepsilon_{\mathrm{num}}} \approx 136.0, \quad 78.0, \quad 45.7,$$

respectively. In all three cases, the empirical hitting probability is $p_{\mathrm{hit}} = 1.000$. For the strongest tested gain pair $(K_1, K_2) = (0.8, 0.02)$, the final empirical disagreement is

$$\widehat{V}_T \approx 1.7345 \cdot 10^{-3}.$$

Thus, the simulations are consistent with the practical fixed-time interpretation of Theorem 1: the stochastic system reaches a small numerical neighborhood of the consensus set after a bounded transient interval.

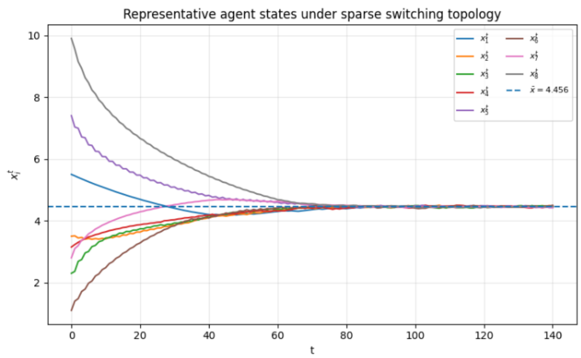

Figure 3. Representative state trajectories under sparse switching topology.

Ablation of the Mixed-Power Mechanism We next examine the role of the two nonlinear components in the proposed local voting protocol. We compare the full mixed-power protocol $(K_1, K_2) = (0.8, 0.02)$, the sublinear-only protocol $(K_1, K_2) = (0.8, 0)$, the cubic-only protocol $(K_1, K_2) = (0, 0.02)$, and the linear voting baseline with $K_L = 0.8$.

The results are shown in Fig. 4.

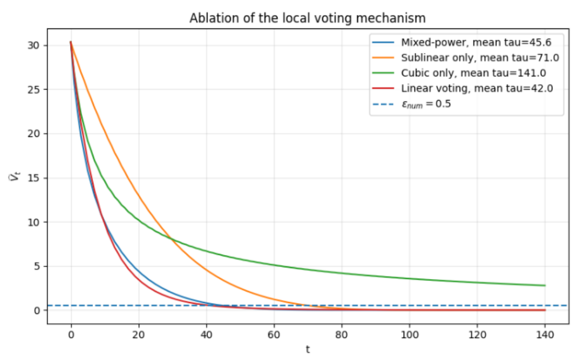

Figure 4. Ablation of the local voting mechanism under sparse switching topology.

The mixed-power protocol reaches the numerical layer faster than the sublinear-only and cubic-only variants. The empirical mean entrance times are

$$45.6, \quad 71.0, \quad 141.0, \quad 42.0,$$

for the mixed-power, sublinear-only, cubic-only, and linear voting protocols, respectively. The cubic-only protocol does not reach the numerical layer on the considered horizon, with $p_{\mathrm{hit}} = 0$. This illustrates the importance of the sublinear term near the consensus manifold.

The linear voting baseline reaches the selected numerical layer slightly faster than the mixed-power protocol for the chosen gain. Therefore, the simulations should not be interpreted as showing that the proposed protocol is the fastest among all baselines. At the same time, the mixed-power protocol yields a smaller final empirical disagreement:

$$\widehat{V}_T^{\mathrm{mixed}} \approx 1.8023 \cdot 10^{-3}, \qquad \widehat{V}_T^{\mathrm{linear}} \approx 3.8965 \cdot 10^{-3}.$$

The empirical mean control efforts for the mixed-power and linear protocols are approximately

$$1.8090 \cdot 10^{-2} \quad \text{and} \quad 1.6297 \cdot 10^{-2},$$

respectively.

Finite-Horizon Trajectory Comparison We next illustrate the trajectory-comparison result of Theorem 2. For each realization of the stochastic system, we simulate the associated ideal exact-measurement trajectory and compute

$$D_t^{(k)} = \frac{1}{2}\|\Pi(X_t^{(k)} - \bar{X}_t)\|^2.$$

The empirical mismatch is then defined by

$$\widehat{D}_t := \frac{1}{N_{\mathrm{MC}}} \sum_{k=1}^{N_{\mathrm{MC}}} D_t^{(k)}.$$

Figure 5 shows $\widehat{D}_t$ for several values of the noise amplitude ρ.

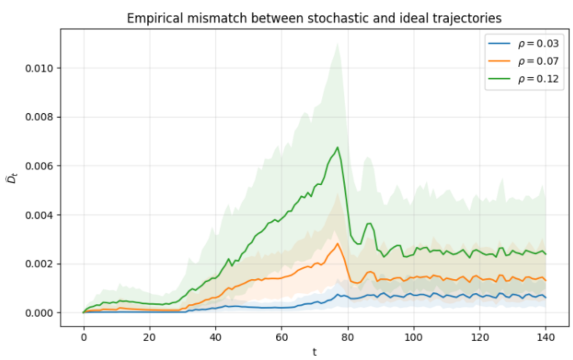

Figure 5. Empirical mismatch $\widehat{D}_t$ between the actual stochastic trajectory and the ideal exact-measurement trajectory for several noise amplitudes ρ, averaged over $N_{\mathrm{MC}} = 200$ runs. The shaded regions indicate empirical 5–95 percentile ranges.

One observes that the actual stochastic trajectory remains close to the ideal exact-measurement one on the considered finite horizon, and that the empirical mismatch becomes smaller as ρ decreases. At the final time, the empirical mismatch values are

$$\widehat{D}_T \approx 6.1184 \cdot 10^{-4}, \quad 1.3113 \cdot 10^{-3}, \quad 2.3856 \cdot 10^{-3}$$

for $\rho = 0.03, 0.07, 0.12$, respectively. This behaviour agrees with the comparison estimate of Theorem 2 and with the fact that the closeness radius vanishes as $\rho \to 0$.

Load-Equalization Interpretation In the present simulations, the state x_i^t is interpreted as a normalized local load level of agent i. The experiment therefore models a static load-equalization scenario: the initial values represent an uneven distribution of load over the network, and the local voting protocol redistributes this imbalance through neighbor interactions. No exogenous arrival process, service process, queue dynamics, or capacity constraints are included in this numerical example. The purpose of the experiment is to illustrate the consensus and trajectory-comparison properties proved above in a load-equalization setting rather than to model a full queueing-based load-balancing system.

Overall, the simulations are consistent with the theory: exact fixed-time consensus is not expected under persistent stochastic perturbations, but the system exhibits practical entrance into a small numerical neighborhood of the consensus manifold together with finite-horizon closeness to the ideal exact-measurement dynamics.

6 Conclusion

This paper studied a stochastic discrete-time multi-agent system with a nonlinear local voting protocol containing signed-power terms of orders $1/3$ and 3. The analysis was carried out in the framework of semi-global practical fixed-time consensus.

Using a disagreement Lyapunov function and a mixed-power drift estimate, we derived a constructive practical consensus radius and a constructive bound on the expected entrance time into the corresponding consensus layer.

We also introduced an ideal exact-measurement comparison system and obtained a finite-horizon bound on the mismatch between the actual stochastic dynamics and the ideal one. This comparison shows that the stochastic trajectory remains close to the ideal trajectory on every fixed finite horizon, with an accuracy that improves as the noise level decreases.

The numerical simulations illustrated the theoretical findings on sparse switching communication graphs. They showed practical entrance into a small neighbourhood of the consensus manifold and demonstrated that the finite-horizon mismatch between the stochastic and ideal trajectories decreases as the noise amplitude becomes smaller.

7 Future Work

Future research may be directed toward extending the proposed framework to more general classes of stochastic disturbances, communication delays, and imperfect information exchange, as well as toward establishing practical fixed-time consensus results under weaker assumptions on the switching interaction topology.

Acknowledgements

Sections 1–2 were carried out with the support of the Herzen State Pedagogical University of Russia (project No. 49VG, "Quality of life of Russian teachers: methodology, theory, measurement methods").

Sections 3–5 were carried out at Saint Petersburg University, project no. 121061000159-6.

References

Amelina, N., Fradkov, A., Jiang, Y., and Vergados, D. J. (2015). Approximate consensus in stochastic networks with application to load balancing. *IEEE Transactions on Information Theory*, **61** (4), pp. 1739–1752.

Amelina, N. O. (2013). Local voting protocol for decentralized load balancing of network with switched topology and noise in measurements. *Vestnik of St. Petersburg University: Mathematics*, **46** (3), pp. 118–125.

Amelina, N. O. and Fradkov, A. L. (2012). Approximate consensus in the dynamic stochastic network with incomplete information and measurement delays. *Automation and Remote Control*, **73** (11), pp. 1765–1783.

Amelina, N. O., Granichin, O. N., and Kornivetc, A. (2013). Local voting protocol in decentralized load balancing problem with switched topology, noise, and delays. In *2013 IEEE 52nd Annual Conference on Decision and Control (CDC)*, IEEE, pp. 4613–4618.

Derevitskii, D. P. and Fradkov, A. L. (1974). Two models for analyzing the dynamics of adaptation algorithms. *Automation and Remote Control*, **35** (1), pp. 59–67.

Erofeeva, V. and Parsegov, S. (2024). Properties of the laplacian spectra of certain basic and hierarchical graphs. *Cybernetics and Physics*, **13** (1), pp. 12–19.

Fu, K., Fu, X., and Li, T. (2025). Distributed dual gradient tracking for nonconvex resource allocation with limited communication data rate. *Cybernetics and Physics*, **14** (1), pp. 40–51.

Galkina, D. and Zhdanov, V. (2024). On finite-time average consensus for three-agent system. In *2024 International Russian Automation Conference (RusAutoCon)*, IEEE, pp. 908–913.

Galkina, D., Zimenko, K., Efimov, D. V., and Polyakov, A. (2025). Stability analysis for homogeneous systems with sector nonlinearities and finite-time average-consensus algorithm for double integrator systems. In *2025 European Control Conference (ECC)*, IEEE, pp. 1231–1236.

Galkina, D. A. (2025). *Razrabotka algoritmov finitnogo upravleniya mul'tiagentnymi sistemami na osnove teorii odnorodnosti*. Candidate of sciences dissertation, ITMO University, Saint Petersburg, Russia.

Ma, L., Liu, Y., et al. (2017). Consensus control of stochastic multi-agent systems: A survey. *Science China Information Sciences*, **60** (12), pp. 120201.

Olfati-Saber, R., Fax, J. A., and Murray, R. M. (2007). Consensus and cooperation in networked multi-agent systems. *Proceedings of the IEEE*, **95** (1), pp. 215–233.

Parsegov, S. E., Polyakov, A. E., and Shcherbakov, P. S. (2013). Fixed-time consensus algorithm for multi-agent systems with integrator dynamics. *IFAC Proceedings Volumes*, **46** (27), pp. 110–115.

Polyakov, A. (2012). Nonlinear feedback design for fixed-time stabilization of linear control systems. *IEEE Transactions on Automatic Control*, **57** (8), pp. 2106–2110.

Polyakov, A., Efimov, D., and Brogliato, B. (2019). Consistent discretization of finite-time and fixed-time stable systems. *SIAM Journal on Control and Optimization*, **57** (1), pp. 78–103.

Polyakov, A., Efimov, D., and Ping, X. (2023). Consistent discretization of homogeneous finite/fixed-time controllers for lti systems. *Automatica*, **155**, pp. 111118.

Sun, F., Lu, C., Zhu, W., and Kurths, J. (2023). Data-sampled mean-square consensus of hybrid multi-agent systems with time-varying delay and multiplicative noises. *Information Sciences*, **624**, pp. 674–685.

Tarasova, E. and Moseiko, E. (2025). Decentralized spsa-based correction of task time predictions in adaptive multi-agent systems. *Cybernetics and Physics*, **14** (1), pp. 67–73.

Vergados, D. J., Amelina, N., Jiang, Y., Kralevska, K., and Granichin, O. (2018). Toward optimal distributed node scheduling in a multihop wireless network through local voting. *IEEE Transactions on Wireless Communications*, **17** (1), pp. 400–414.

Zhang, L., Zhang, H., and Xie, L. (2024). Mean-square output consensus for heterogeneous multi-agent systems over nonidentical packet loss channels. *Automatica*, **160**, pp. 111463.

Zhang, R., Zhang, Y., and Zong, X. (2022). Stochastic leader-following consensus of discrete-time nonlinear multi-agent systems with multiplicative noises. *Journal of the Franklin Institute*, **359** (14), pp. 7753–7774.